Graph-based topology retrieval and constructive solid geometry for structural BIM refinement

Muataz S. A. Albadri[1], Patricia González-Cabaleiro[1], Antonio Fernández[1], Lucía Díaz-Vilariño[1]

[1]CINTECX, Universidade de Vigo, GeoTECH group, 36310 Vigo, Spain
(muatazsafaaabed.albadri, patricia.gonzalez.cabaleiro, antfdez, lucia)@uvigo.gal

Keywords: Scan-to-BIM, as-built BIM, IFC, CSG, connectivity graph, automatic modelling.

Abstract

As-built Building Information Models (BIMs) are crucial for building digitalisation, structural analysis, and life cycle management. Despite recent advances, automated reconstruction of structural elements from point clouds remains a challenging task, particularly in ensuring geometric accuracy and topological consistency within a storey and across consecutive storeys. This paper proposes an automated method for refining topological inconsistency between columns, beams, and slabs, ensuring consistent as-built BIMs. The method places Constructive Solid Geometry (CSG) at the core of refinement process, driven by fundamental structural principles. The method starts by creating solid rectangular prisms from labelled point clouds. Beams are then aligned both vertically and horizontally within each storey. Columns are vertically aligned across consecutive storeys. Topology relationships between the elements are retrieved and encoded in graphs. These graphs, together with a set of Boolean operations, are used to resolve gaps and trim overlaps between the connected elements. The refined elements are represented in accordance with the IFC standards. The proposed method was validated on two multi-storey case studies representing frame and flat-slab building structures. Both qualitative and quantitative evaluations confirmed the effectiveness of the approach, achieving significant geometric accuracy and topological consistency. In addition, the method exhibits efficient runtime performance, indicating its promise for scalable Scan-to-BIM automation.

1. Introduction

Concrete buildings are typically composed of structural elements, such as columns, beams, and slabs, that ensure load transfer safely to the foundation. Accurate digital representations of existing buildings are essential for supporting documentation, maintenance, and assessment within BIM workflows. In this context, recent advances in 3D data acquisition technologies significantly accelerated the development of Scan-to-BIM methodologies. Typical Scan-to-BIM workflows rely on processing point cloud data to detect building elements followed by extracting geometric features and spatial relationships to reconstruct as-built models. Although current techniques achieve substantial progress in terms of geometric accuracy and automation, preserving topological consistency among the elements remains a critical challenge (Noichl et al., 2025, Reisinger et al., 2025). In current techniques, structural elements are usually segmented and reconstructed independently, which frequently results in overlaps or gaps among them (Yang et al., 2017). These topological deficiencies undermine the reliability of reconstructed BIMs, limiting their applicability for building analysis, interoperability, and integration into advanced digital environments. Considering these limitations, this paper aims to automatically reconstruct consistent BIMs of the structural elements from segmented point clouds, focusing on the automatic refinement of the topological inconsistency such as misalignment, overlaps, and gaps.

Recently, numerous methods have been proposed for point cloud segmentation, advancing automation and generalisability in extracting building elements from 3D data (Díaz-Vilariño et al., 2015, Son and Kim, 2017, Truong-Hong and Lindenbergh, 2022, Wang and Kim, 2019). These methods establish a crucial foundation for the subsequent geometric and topological reconstruction of buildings. Existing studies have addressed the reconstruction of structural elements, achieving promising results on their case studies (Abreu et al., 2023, Kim and Kim, 2021, Tran and Khoshelham, 2020). However, more robust reconstruction methods that explicitly preserve topological consistency are still needed. Reconstruction techniques can be categorized, based on their implicit representations, into three main groups: Boundary Representation (B-rep), Swept Solid Representation (SSR), and Constructive Solid Geometry (CSG) (Tang et al., 2010). The B-rep-based techniques represent the building elements through their faces, edges, and vertices. In contrast, the SSR-based methods represent the elements using their cross-sectional profiles and extrusion directions. However, both B-rep- and SSR- methods generally require extracting geometric and topological information from point clouds to achieve consistent as-built BIMs (Gourguechon et al., 2022, Ochmann et al., 2016, Roman et al., 2024, Tang et al., 2022).

CSG-based methods represent complex geometries with the advantage of topology preservation. Such approaches apply Boolean operations (e.g., *union*, *Intersection*, and *Difference*) to basic primitives, such as rectangular prisms, producing solid geometries (Fayolle and Friedrich, 2024). The CSG is widely adopted in Computer-Aided Design (CAD) and 3D computer graphics (Chen et al., 2024, Yin et al., 2020, Yin et al., 2020). For instance, a CSG-based method was developed to reconstruct the solid geometries of mechanical parts, furniture, and urban scenes by extracting primitives from point clouds and applying Boolean operations (Wu et al., 2018). The CSG was also used for reconstructing indoor scenes of museums from point clouds (Xiao and Furukawa, 2014). Similarly, (Albadri et al., 2025) proposed an automated CSG-based method to reconstruct as-built BIM from point clods. The proposed method begins by generating solid primitives for rooms, doors, and openings, followed by the application of a set of Boolean operations to reconstruct the solid geometries of building elements, including slabs, walls, doors, windows, and indoor spaces. The resulting elements are represented in accordance with the IFC standard, producing topologically consistent as-built BIMs. (Rausch and Haas, 2021) proposed a parametric CSG-based approach to update the geometry of building elements to match as-built point clouds. They demonstrated the robustness of CSG to missing point cloud data and its effectiveness in preserving the geometry of individual elements. However, topological consistency among elements was not considered in the proposed approach, and preserving such relationships would require additional parametric optimisation processes.

Retrieval of topological relationships, particularly between structural elements, is fundamental for reliable as-built BIMs (Sampaio and Gomes, 2021, Tang et al., 2010). For instance, connectivity relationships enable the accurate identification of the load-bearing hierarchy among the elements. The connection between a column and a beam typically refers to a support relationship, where the column transfers loads from the beam (Nguyen et al., 2005). Similarly, columns act as primary vertical supports for a slab that connects with them, in case of flat-slab buildings (i.e., without beams). In this context, the topological relationships are identified and encoded through graph-based representations, where nodes represent elements and edges represent the relations between them (Gordon et al., 2023).

This paper proposes an automated CSG-based method for the reconstruction of structural elements from labelled point clouds, ensuring both geometric accuracy and topological consistency among the elements. The CSG, driven by fundamental structural principles, is used to retrieve connectivity graphs, which represent meaningful relationships between the elements, including connection and support relationships. These relationships, together with Boolean operations, are used to address misalignment, overlaps, and gaps between the connected elements. The refined elements are finally represented in compliance with the IFC schema, producing topologically consistent as-built BIMs.

The rest of the paper is organized as follows. Section 2 explains the proposed method. Results are presented in Section 3. Section 4 demonstrates evaluation and discussion. Finally, section 5 summarizes the conclusion of this work.

2. Method

The proposed method is based on the load-transfer principles governing reinforced concrete buildings, where columns transfer loads from slabs and beams. In multi-storey buildings, columns are the primary elements that transfer loads between storeys. It is worth pointing out that this study assumes that the buildings comply with Manhattan constraints and the structural elements possess rectangular cross-sections. These principles are embedded within the rules of the proposed method, ensuring columns continuity across storeys while beams and slabs are trimmed at their supporting columns.

The proposed method is illustrated in Figure 1. The input data consists of labelled point clouds (PCD) of elements, including columns, beams, and slabs. The method starts by extracting the bounding box of each element from the PCD. The base profile (B) is then identified by the XY coordinates corresponding to the lowest Z value of the bounding box, representing the element's cross-sectional footprint. The base's dimensions are approximated based on design standards of the structural elements, reflecting the use of regular dimensional increments in practical construction (e.g., multiples of 5 cm in this study). In parallel, the height of the element is determined as the difference between the maximum and minimum Z values of its bounding box. Subsequently, the projected base (B) is extruded along the vertical direction considering the element's height, resulting in a solid rectangular prism of each element.

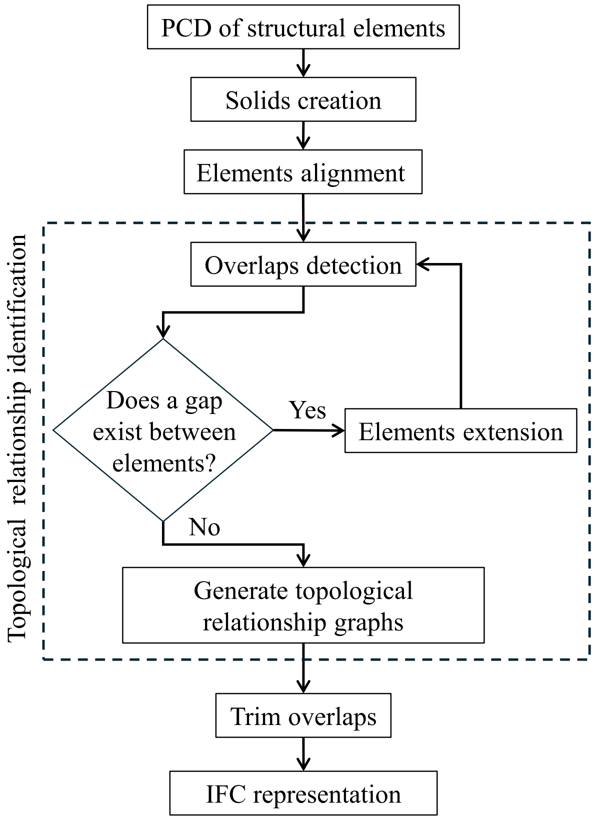

Figure 1. The proposed method for the reconstruction of consistent structural elements.

An alignment process is applied to columns and to beams for mitigating deviations introduced during the solid creation stage. Columns are aligned vertically across consecutive storeys. To this end, the base profiles of all columns are projected onto the XY plane, and the intersection-over-union (IoU) is computed between the projected bases, as defined in Equation 1. Column pairs are identified as candidates for alignment when the computed IoU exceeds a predefined threshold (IoU_{th}). For each candidate pair, the column with the larger projected base area is selected as the reference, while the remaining column is translated horizontally such that its centroid coincides with the centroid of the reference column.

$$\text{IoU} = \frac{I}{U} \tag{1}$$

where I denotes the area of intersection between the projected base profiles of two columns on the XY plane, and U denotes the area of their union.

Beams are aligned within each storey through a two-step process: top-Z alignment and transverse alignment. In the top-Z alignment, the maximum Z value among all beams in a storey is identified. The beams are vertically translated to ensure alignment of their top Z coordinates with the maximum Z value. For transverse alignment, beams are first classified according to their longitudinal axis into X-oriented and Y-oriented groups. Within each group, their bounding boxes are projected onto the plane orthogonal to the longitudinal axis. The IoU values are also computed between these projections. Similar to the column alignment process, beams with an IoU exceeding the IoU_{th} are identified as beams to be aligned. The beam with the largest projected area is defined as the reference, and the rest of the beams are horizontally translated so that their centroids align with the centroid of the reference beam.

The retrieval of topological relationships proceeds by first detecting overlaps between the elements using the *Intersection* operation. Beam–beam, column–beam, and column–slab overlaps indicate connectivity (classified as *connected elements*), while the absence of overlap denotes disconnection (classified as *disconnected elements*). However, the *disconnected elements* may include elements that should be connected, potentially resulting in incomplete topology; therefore, an element-extension step is proposed in this study. The element-extension step is applied to the *disconnected elements* to resolve gaps between structural elements. The gaps are characterized by computing the minimum Euclidean distance between the elements. Element pairs with gaps below a predefined threshold (d_{th}) are classified as *potentially connected elements*, which are then extended along their principal axis by a distance d, as defined in Equation 2. This extension process is performed iteratively, with the classifications of *connected* and *disconnected elements* updated at each iteration. Extension for a given element is terminated once its accumulated extension distance reaches the threshold (d_{th}). Finally, beams that overlap with other beams are classified as *connected beams*, and columns that intersect with beams or slabs are identified as *supporting columns* for those elements, reflecting support relationships. These relationships are subsequently preserved for refinement operations.

$$d = \begin{cases} t_c, & \text{if the extending element is a beam,} \\ t_b, & \text{if the extending element is a column.} \end{cases} \quad (2)$$

where t_c denotes the column thickness, which is obtained as the smaller horizontal dimension of a column, and t_b denotes the beam depth, which is identified as the vertical dimension of a beam. For flat-slab buildings t_b denotes the slab depth.

The retrieved relationships are encoded in four graphs: beam-beam connection graph ($G_{b\text{-}b}$), column-beam support graph ($G_{c\text{-}b}$), column-slab support graph ($G_{c\text{-}s}$), and column-column support graph ($G_{c\text{-}c}$). In all graphs, the nodes represent the elements and the edges denote the connectivity relationships between the elements. A trimming process is then applied to cut the overlaps between the connected elements based on the retrieved relationship graphs. For each pair in $G_{b\text{-}b}$, the overlap is trimmed from only one beam, the beam with the smaller cross-section area, using the *Difference* operator. For each pair in $G_{c\text{-}b}$, the overlaps between beams and their supporting column are cut from the beams, resulting in beams trimmed at the column faces. Slabs are similarly trimmed by their supporting columns, ensuring that columns remain continuous through the slabs to the upper storeys. Finally, for each pair in $G_{c\text{-}c}$, the overlaps between the columns are trimmed from the columns in upper storey. The resulting elements are mapped to the corresponding IFC entities, including *IfcColumn*, *IfcBeam*, and *IfcSlab*, resulting in a refined as-built BIM that is compliant with the IFC standards.

3. Results

Two case studies were used to validate the proposed method in this study, including simulated and real-world scenarios. Both case studies comply with the Manhattan-world constraints, and all elements exhibit rectangular cross-sections. The simulated case study (CS1) represents a two-storey building, containing 40 columns and 57 beams. In contrast, the real-world case study (CS2) represent a flat-slab building, comprising 48 columns and 3 slabs. The input data consists of segmented point clouds (PCD) of structural elements, columns and beams for CS1, and columns and slabs for CS2, as shown in Figure 2a. The PCD contain overlaps and disconnections between neighbouring elements, reflecting realistic reconstruction challenges (Figure 3a). The method was implemented in Python 3.11 using FreeCAD API (version 1.0.0) and *IfcOpenShell*.

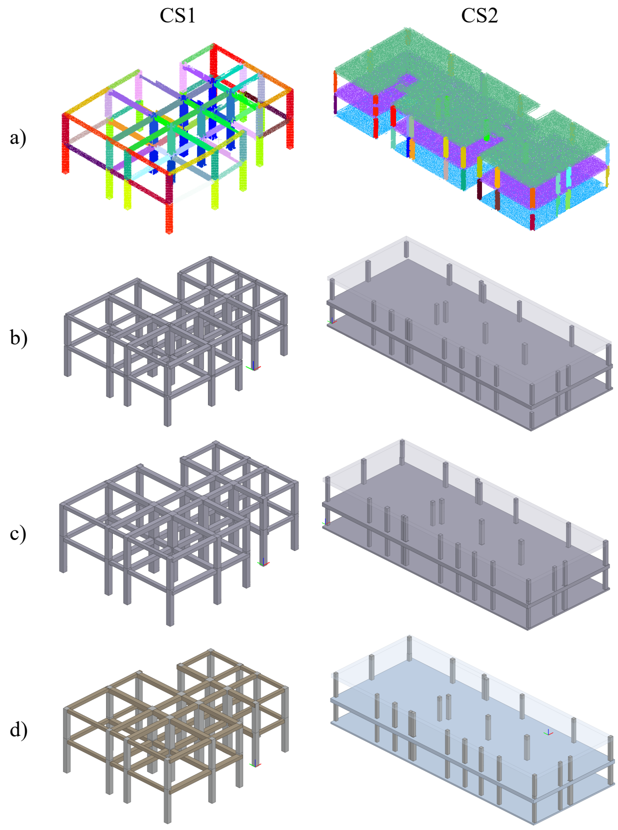

Figure 2. Input data and results. a) Segmented point clouds of columns and beams (CS1) and columns and slabs (CS2); b) initially reconstructed solids of the elements; c) refined elements; and d) IFC models. The upper slab of CS2 is shown as transparent for improved visualization.

Solids of the elements were first created, as illustrated in Figure 2b. At this stage, topology inconsistency is evident among the elements (Figure 3b). In CS1, beams overlap or disconnect with their supporting columns. CS2 contains columns overlapping or disconnecting with slabs. Moreover, elements exhibit misalignment in both case studies.

The elements were aligned by setting the threshold value of IoU_{th} as 0.5. Alternative values (0.1, 0.3, 0.7, and 0.9) were

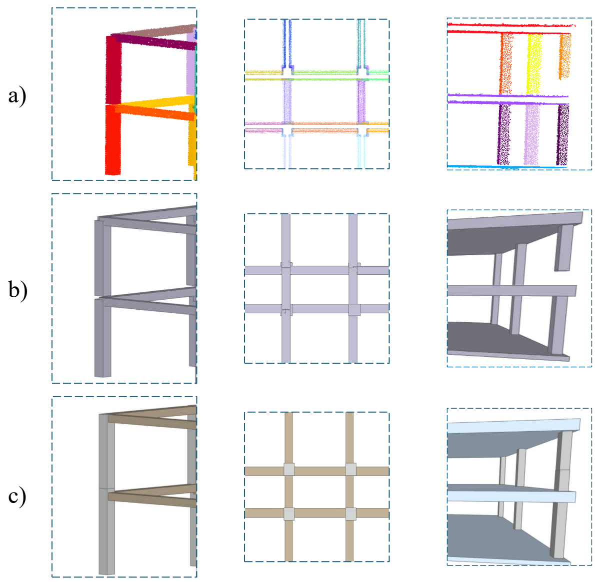

Figure 3. Topology preservation among structural elements: (a) Segmented point clouds, (b) initially reconstructed solids, and (c) refined IFC models.

also tested. The alignment results remained mostly unaffected with the values of 0.1 and 0.3; however, using 0.7 and 0.9 values resulted in some elements not being aligned. This behaviour is expected, as the misaligned elements exhibit low IoU values. Furthermore, the IoU_{th} can be adjusted to a smaller value, allowing all elements intended for alignment to be correctly aligned across diverse building configurations.

Topological relationships were identified and encoded in graphs (Figures 4 and 5), by setting the threshold distance (d_{th}) as 1.5 metres in both case studies. Alternative threshold values (0.5, 1.0, and 2.0) metres were also tested. Using d_{th} = 2.0 resulted in the same relationships being identified. In contrast, setting d_{th} to smaller values (0.5 and 1.0) resulted in some relationships between elements not being identified, particularly when large gaps were present.

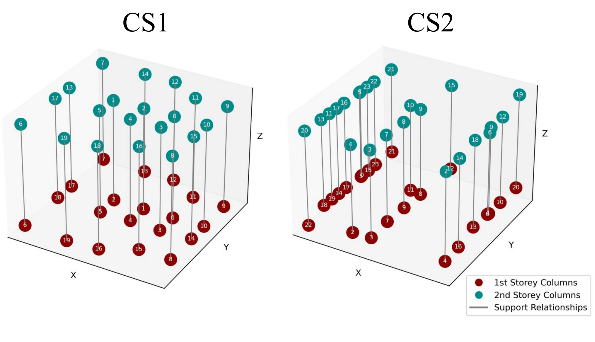

Figure 4. Column-column support graphs $G_{c\text{-}c}$ for CS1 and CS2.

Figure 4 illustrates the column-column relationships for CS1 and CS2. In these graphs, all columns in the upper storey are connected to the corresponding columns in the lower storey, effectively demonstrating their dependencies. Similarly, column-beam graphs were created for both storeys of CS1, as shown in Figure 5a, where each column is correctly connected with the beams it supports. Beam-beam connection graphs, shown in Figure 5b, effectively illustrate the continuity and interconnections of beams within each storey.

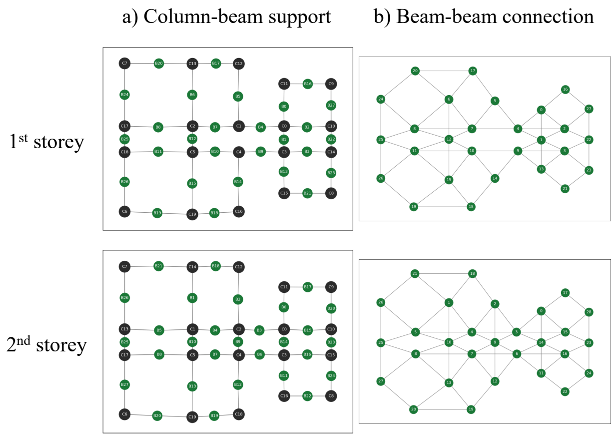

Figure 5. Topological relationships of columns and beams for CS1. a) Column-beam support graphs $G_{c\text{-}b}$ and b) Beam-beam connection graphs $G_{b\text{-}b}$.

Topology inconsistency were successfully resolved across the structural elements in both case studies (Figures 2c and 3c). IFC models were also created, representing consistent as-built BIMs for both types of buildings (Figure 2d).

4. Evaluation and Discussion

The retrieved topological relationships provided critical insight into the connectivity and load-transfer hierarchy of the elements, allowing for systematic refinement of overlaps, gaps, and misalignments. The results demonstrate the effectiveness of the proposed method in refining topology among the structural elements both within individual storeys and across consecutive storeys, for both frame and flat-slab buildings. Beams and slabs are correctly trimmed with respect to their supporting columns, successfully resolving common modelling challenges, overlaps and gaps, as shown in Figure 3.

Although the method achieves significant performance, certain challenges remain. For column–column topology, the columns are currently trimmed at the contact surface after extending the columns from the storey below. This may result in columns from the lower storey extending into the upper storey when a gap exists in the upper column (Figure 3). Ideally, columns should be trimmed at the level of the slab between consecutive storeys to ensure that each column is fully contained within its respective storey.

For column–beam topology, some beams remain continuous alongside their supporting column, as illustrated in Figure 6a, because these beams with widths exceeding the width of the column or because they are not fully aligned with the column. However, beams should be terminated at the contact surface of their supporting column, orthogonal to the beam’s principal axis. On the other hand, column-slab topology is effectively reconstructed using the proposed approach Figure 6b; however, the method can be developed to allow control over whether the overlap is trimmed from the slabs or the columns. These modifications could improve flexibility and accuracy of the topology refinement process.

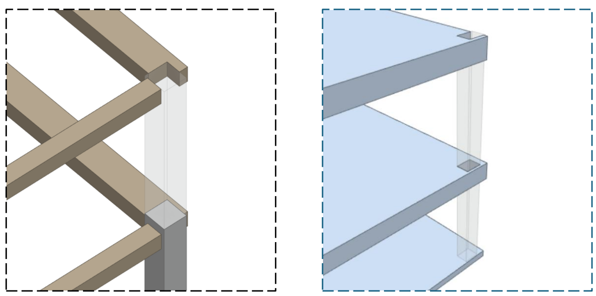

Figure 6. The overlap trimming applied to (a) beams and (b) slabs.

The geometry of the reconstructed models is also evaluated in this study. A point-to-model approach was used to evaluate how accurately the reconstructed geometry represents the input PCD. For the evaluation, the reconstructed IFC model was first converted into a unified mesh, which was then uniformly sampled to generate points representing the model surfaces. For each point in PCD, the Euclidean distance (e) to the nearest point on the sampled mesh was calculated.

Figure 7 shows the point-to-model evaluation results for both case studies. These distances were subsequently analysed to obtain quantitative metrics, including mean absolute deviation (Mean), root mean square deviation (RMS), and Standard deviation (σ). The metrics are computed as defined in Equations 3, 4, and 5.

$$\text{Mean} = \frac{1}{N}\sum_{i=1}^{N} e_i \tag{3}$$

$$\text{RMS} = \sqrt{\frac{1}{N}\sum_{i=1}^{N} e_i^2} \tag{4}$$

$$\sigma = \sqrt{\frac{1}{N}\sum_{i=1}^{N} (e_i - Mean)^2} \tag{5}$$

where e_i denotes the Euclidean distance between the i-th point of the PCD and its nearest point on the sampled mesh, and N is the total number of evaluated points.

The quantitative evaluation results are presented in Table 1. For CS1, the overall deviations are relatively low (Mean = 5.3 cm), although local deviations are slightly more dispersed ($\sigma = 4.3$ cm). For CS2, the deviations are more consistent across the reconstructed elements ($\sigma = 1.9$ cm), although the Mean and RMS are relatively higher, at 7.7 cm and 8.0 cm, respectively. Despite these deviations, the overall deviation magnitudes remain within acceptable limits for as-built BIM applications. The geometric reconstruction accuracy could be further improved by employing more advanced vertex extraction techniques, thereby reducing reliance on bounding box approximations.

Overall, the study demonstrates that integrating domain-knowledge-based rules with CSG enables the automated reconstruction of structural elements while consistently preserving both geometry and topology. In terms of computational performance, the complete processing time required approximately 1 minute for CS1 and 15 seconds for CS2, executed on a personal computer equipped with an NVIDIA RTX 4070 GPU and 32 GB of RAM.

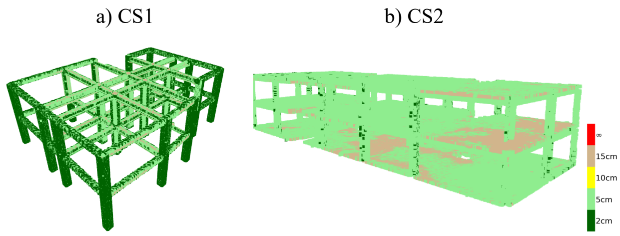

Figure 7. Point-to-model evaluation results for CS1 (a) and CS2 (b).

	CS1	CS2
Mean	5.3 cm	7.7 cm
RMS	6.8 cm	8.0 cm
σ	4.3 cm	1.9 cm

Table 1. Quantitative evaluation results.

5. Conclusion

This study introduces an automated CSG-based method for addressing topological inconsistency in the reconstruction of structural elements from point clouds. By integrating CSG with fundamental structural principles, topological relationships between columns, beams and slabs are identified and encoded within graphs. These relationships are used to guide the application of Boolean operations for refining topology, systematically resolving misalignments, overlaps, and gaps between the elements. The refined elements are finally represented in compliance with the IFC schema, resulting in topologically consistent and semantically enriched BIMs.

The proposed method was validated using two multi-storey buildings, including frame and flat-slab structures. The results demonstrate the method's capability to accurately reconstruct buildings while preserving topology among the elements within and across consecutive storeys. A quantitative point-to-model evaluation confirmed a high level of geometric agreement between the input point clouds and the reconstructed IFC models, with mean deviations remaining below 8 cm. Furthermore, key topological relationships, including column–column, column–beam, and beam–beam relations, were effectively identified and preserved in graphs, producing reliable as-built information suitable for building analysis and digital twin development.

Although the method demonstrate significant performance, challenges remain. In particular, the trimming process could be further enhanced to improve flexibility and accuracy in topology refinement under more complex building configurations. Future works therefore will focus on improving scalability and generalisability, including the handling of non-Manhattan-world buildings and elements with non-rectangular cross-sections, such as circular or hexagonal columns.

Acknowledgment

This is work was partially supported by human resources grant RYC2020-029193-I funded by MCIN/AEI/10.13039/501100011033 and FSE ‘El FSE invierte en tu futuro’, by grant ED431F 2022/08 funded by Xunta de Galicia, Spain-GAIN, and by the projects PID2021-123475OA-I00 funded by MCIN/AEI /10.13039/501100011033/ and by FEDER ‘Una manera de hacer Europa’ and CNS2022-135730 funded by MCIN/AEI /10.13039/501100011033 and by European Union NextGenerationEU/PRTR. The statements made herein are solely the responsibility of the authors.

References

Abreu, N., Pinto, A., Matos, A., Pires, M., 2023. Procedural point cloud modelling in Scan-to-BIM and Scan-vs-BIM applications: A Review. *ISPRS International Journal of Geo-Information*, 12(7). doi.org/10.3390/ijgi12070260.

Albadri, M. S. A., González-Cabaleiro, P., Fernández, A., Díaz-Vilariño, L., 2025. Exploring constructive solid geometry for building reconstruction from point clouds: Preliminary results. *The International Archives of the Photogrammetry, Remote Sensing and Spatial Information Sciences*, 48, 1-7. doi.org/10.5194/isprs-archives-XLVIII-4-W15-2025-1-2025.

Chen, J., Shen, Z., Zhao, M., Jia, X., Yan, D.-M., Wang, W., 2024. FR-CSG: Fast and reliable modeling for constructive solid geometry. *IEEE Transactions on Visualization and Computer Graphics*, 1-15. doi.org/10.1109/TVCG.2024.3481278.

Díaz-Vilariño, L., Conde, B., Lagüela, S., Lorenzo, H., 2015. Automatic detection and segmentation of columns in as-built buildings from point clouds. *Remote Sensing*, 7(11), 15667. doi.org/10.3390/rs71115651.

Fayolle, P.-A., Friedrich, M., 2024. A survey of methods for converting unstructured data to CSG models. *Computer-Aided Design*, 168, 103655. doi.org/10.1016/j.cad.2023.103655.

Gordon, M., Batallé, A., Wolf, C. D., Sollazzo, A., Dubor, A., Wang, T., 2023. Automating building element detection for deconstruction planning and material reuse: A case study. *Automation in Construction*, 146, 104697. doi.org/10.1016/j.autcon.2022.104697.

Gourguechon, C., Macher, H., Landes, T., 2022. Automation of as-built BIM creation from point cloud: An overview of research works focused on indoor environment. *The International Archives of the Photogrammetry, Remote Sensing and Spatial Information Sciences*, XLIII-B2-2022, 193-200. doi.org/10.5194/isprs-archives-XLIII-B2-2022-193-2022.

Kim, H., Kim, C., 2021. 3D as-built modeling from incomplete point clouds using connectivity relations. *Automation in Construction*, 130, 103855. doi.org/10.1016/j.autcon.2021.103855.

Nguyen, T.-H., Oloufa, A. A., Nassar, K., 2005. Algorithms for automated deduction of topological information. *Automation in Construction*, 14(1), 59-70. doi.org/10.1016/j.autcon.2004.07.015.

Noichl, F., Pan, Y., Borrmann, A., 2025. Automated steel structure model reconstruction through point cloud instance segmentation and parametric shape fitting. *Journal of Information Technology in Construction*, 30, 1099-1122. doi.org/10.36680/j.itcon.2025.045.

Ochmann, S., Vock, R., Wessel, R., Klein, R., 2016. Automatic reconstruction of parametric building models from indoor point clouds. *Computers & Graphics*, 54, 94-103. doi.org/10.1016/j.cag.2015.07.008.

Rausch, C., Haas, C., 2021. Automated shape and pose updating of building information model elements from 3D point clouds. *Automation in Construction*, 124, 103561. doi.org/10.1016/j.autcon.2021.103561.

Reisinger, J., Marin, D., Rufinatscha, P., Kan, P., 2025. Scan2Beams: Moving towards automated modelling and analysis of structural industrial building stock. *International Council for Research and Innovation in Building and Construction*. doi.org/10.35490/EC3.2025.194.

Roman, O., Mazzacca, G., Farella, E. M., Remondino, F., Bassier, M., Agugiaro, G., 2024. Towards automated BIM and BEM model generation using a B-Rep-based method with Topological Map. *ISPRS Annals of the Photogrammetry, Remote Sensing and Spatial Information Sciences*, X-4-2024, 287-294. doi.org/10.5194/isprs-annals-X-4-2024-287-2024.

Sampaio, A. Z., Gomes, A. M., 2021. BIM interoperability analyses in structure design. *CivilEng*, 2(1), 192. doi.org/10.3390/civileng2010010.

Son, H., Kim, C., 2017. Semantic as-built 3D modeling of structural elements of buildings based on local concavity and convexity. *Advanced Engineering Informatics*, 34, 114-124. doi.org/10.1016/j.aei.2017.10.001.

Tang, P., Huber, D., Akinci, B., Lipman, R., Lytle, A., 2010. Automatic reconstruction of as-built building information models from laser-scanned point clouds: A review of related techniques. *Automation in Construction*, 19(7), 829-843. doi.org/10.1016/j.autcon.2010.06.007.

Tang, S., Li, X., Zheng, X., Wu, B., Wang, W., Zhang, Y., 2022. BIM generation from 3D point clouds by combining 3D deep learning and improved morphological approach. *Automation in Construction*, 141, 104422. doi.org/10.1016/j.autcon.2022.104422.

Tran, H., Khoshelham, K., 2020. Procedural reconstruction of 3D indoor models from lidar data using reversible jump markov chain monte carlo. *Remote Sensing*, 12(5). doi.org/10.3390/rs12050838.

Truong-Hong, L., Lindenbergh, R., 2022. Extracting structural components of concrete buildings from laser scanning point clouds from construction sites. *Advanced Engineering Informatics*, 51, 101490. doi.org/10.1016/j.aei.2021.101490.

Wang, Q., Kim, M.-K., 2019. Applications of 3D point cloud data in the construction industry: A fifteen-year review from 2004 to 2018. *Advanced Engineering Informatics*, 39, 306-319. doi.org/10.1016/j.aei.2019.02.007.

Wu, Q., Xu, K., Wang, J., 2018. Constructing 3D CSG models from 3D raw point clouds. *Computer Graphics Forum*, 37, Wiley Online Library, 221–232. doi.org/10.1111/cgf.13504.

Xiao, J., Furukawa, Y., 2014. Reconstructing the world’s museums. *International Journal of Computer Vision*, 110(3), 243-258. doi.org/10.1007/s11263-014-0711-y.

Yang, X., Koehl, M., Grussenmeyer, P., 2017. Parametric modelling of as-built beam framed structure in BIM environment. *The International Archives of the Photogrammetry, Remote Sensing and Spatial Information Sciences*, 42, 651-657. doi.org/10.5194/isprs-archives-XLII-2-W3-651-2017.

Yin, G., Xiao, X., Cirak, F., 2020. Topologically robust CAD model generation for structural optimisation. *Computer Methods in Applied Mechanics and Engineering*, 369, 113102. doi.org/10.1016/j.cma.2020.113102.